Pulse train fluorescence technique for measuring triplet state dynamics

Leonardo De Boni,[1,*] Paulo L. Franzen,[1] Pablo J. Gonçalves,[2] Iouri E. Borissevitch,[3] Lino Misoguti,[1] Cleber R. Mendonça,[1] and Sergio C. Zilio[1]

[1]*Instituto de Física de São Carlos, Universidade de São Paulo, CP 369, 13560-970 São Carlos, SP, Brasil*
[2]*Instituto de Física, Universidade Federal de Goiás, Caixa Postal 131, 74001-970 Goiânia, GO, Brazil*
[3]*Departamento de Física e Matemática, FFLCRP, Universidade de São Paulo, Av. Bandeirantes 3900, 14040-90, Ribeirão Preto, SP, Brazil*
**deboni@ifsc.usp.br*

Abstract: We report on a method to study the dynamics of triplet formation based on the fluorescence signal produced by a pulse train. Basically, the pulse train acts as sequential pump-probe pulses that precisely map the excited-state dynamics in the long time scale. This allows characterizing those processes that affect the population evolution of the first excited singlet state, whose decay gives rise to the fluorescence. The technique was proven to be valuable to measure parameters of triplet formation in organic molecules. Additionally, this single beam technique has the advantages of simplicity, low noise and background-free signal detection.

OCIS codes: (190.4400) Nonlinear optics, materials; (300.2530) Fluorescence, laser-induced.

References and links

1. B. W. Pogue, T. Momma, H. C. Wu, and T. Hasan, "Transient absorption changes in vivo during photodynamic therapy with pulsed-laser light," Br. J. Cancer **80**(3-4), 344–351 (1999).
2. M. E. Thompson, "The evolution of organometallic complexes in organic light-emitting devices," Mater. Res. Bull. **32**(09), 694–701 (2007).
3. B. W. Pogue, B. Ortel, N. Chen, R. W. Redmond, and T. Hasan, "A photobiological and photophysical-based study of phototoxicity of two chlorins," Cancer Res. **61**(2), 717–724 (2001).
4. W. R. Dawson and M. Windsor, "An eye protective panel for flash-blindness protection using triplet state photochromism," Appl. Opt. **8**(5), 1045–1050 (1969).
5. P. Miles, "Bottleneck optical pulse limiters revisited," Appl. Opt. **38**(3), 566–570 (1999).
6. J. H. Chou, M. E. Kosal, H. S. Nalwa, N. A. Rakow, and K. S. Suslick, "Applications of porphyrins and metalloporphyrins to materials chemistry," in *The Porphyrin Handbook*, K. Kadish, K. Smith, and R. Guillard, eds. (Academic Press, 2000), Chap. 41.
7. S. Haneder, E. Da Como, J. Feldmann, J. M. Lupton, C. Lennartz, P. Erk, E. Fuchs, O. Molt, I. Munster, C. Schildknecht, and G. Wagenblast, "Controlling the radiative rate of deep-blue electrophosphorescent organometallic complexes by singlet-triplet gap engineering," Adv. Mater. (Deerfield Beach Fla.) **20**(17), 3325–3330 (2008).
8. T. G. Pavlopoulos, "Measurement of molar triplet extinction coefficients of organic-molecules by means of cw laser excitation," J. Opt. Soc. Am. **63**(2), 180–184 (1973).
9. S. Speiser and M. Orenstein, "Spatial light modulation via optically induced absorption changes in molecules," Appl. Opt. **27**(14), 2944–2948 (1988).
10. A. R. Horrocks, T. Medinger, and F. Wilkinson, "Solvent dependence of quantum yield of triplet state production of 9-phenylanthracene," Photochem. Photobiol. **6**(1), 21–28 (1967).
11. G. Burdzinski, M. Bayda, G. L. Hug, M. Majchrzak, B. Marciniec, and B. Marciniak, "Time-resolved studies on the photoisomerization of a phenylene-silylene-vinylene type compound in its first singlet excited state," J. Lumin. **131**(4), 577–580 (2011).
12. M. Pineiro, A. L. Carvalho, M. M. Pereira, A. M. R. Gonsalves, L. G. Arnaut, and S. J. Formosinho, "Photoacoustic measurements of porphyrin triplet-state quantum yields and singlet-oxygen efficiencies," Chemistry **4**(11), 2299–2307 (1998).
13. B. Fletcher and J. J. Grabowski, "Photoacoustic calorimetry—an undergraduate physical-organic experiment," J. Chem. Educ. **77**(5), 640–645 (2000).
14. Y. Harada, T. Suzuki, T. Ichimura, and Y. Z. Xu, "Triplet formation of 4-thiothymidine and its photosensitization to oxygen studied by time-resolved thermal lensing technique," J. Phys. Chem. B **111**(19), 5518–5524 (2007).

#144955 - $15.00 USD Received 28 Mar 2011; revised 14 May 2011; accepted 15 May 2011; published 18 May 2011

15. T. Suzuki, U. Okuyama, and T. Ichimura, "Double proton transfer reaction of 7-azaindole dimer and complexes studied by time-resolved thermal lensing technique," J. Phys. Chem. A **101**(38), 7047–7052 (1997).
16. L. Misoguti, C. R. Mendonca, and S. C. Zilio, "Characterization of dynamic optical nonlinearities with pulse trains," Appl. Phys. Lett. **74**(11), 1531–1533 (1999).
17. C. R. Mendonça, L. Gaffo, L. Misoguti, W. C. Moreira, O. N. Oliveira, Jr., and S. C. Zilio, "Characterization of dynamic optical nonlinearities in ytterbium bis-phthalocyanine solution," Chem. Phys. Lett. **323**(3-4), 300–304 (2000).
18. P. Goncalves, L. Boni, N. Neto, J. Rodrigues, Jr., S. Zilio, and I. Borissevitch, "Effect of protonation on the photophysical properties of meso-tetra(sulfonatophenyl) porphyrin," Chem. Phys. Lett. **407**(1-3), 236–241 (2005).
19. P. J. Gonçalves, L. P. F. Aggarwal, C. A. Marquezin, A. S. Ito, L. De Boni, N. M. B. Neto, J. J. Rodrigues, Jr., S. C. Zilio, and I. E. Borissevitch, "Effects of interaction with CTAB micelles on photophysical characteristics of meso-tetrakis(sulfonatophenyl) porphyrin," J. Photochem. Photobiol., A **181**(2-3), 378–384 (2006).
20. P. J. Gonçalves, L. De Boni, I. E. Borissevitch, and S. C. Zílio, "Excited state dynamics of meso-tetra(sulphonatophenyl) metalloporphyrins," J. Phys. Chem. A **112**(29), 6522–6526 (2008).
21. P. L. Franzen, L. Misoguti, and S. C. Zilio, "Hyper-Rayleigh scattering with picosecond pulse trains," Appl. Opt. **47**(10), 1443–1446 (2008).
22. S. Reindl and A. Penzkofer, "Triplet quantum yield determination by picosecond laser double-pulse fluorescence excitation," Chem. Phys. **213**(1-3), 429–438 (1996).
23. S. Reindl and A. Penzkofer, "Higher excited-state triplet-singlet intersystem crossing of some organic dyes," Chem. Phys. **211**(1-3), 431–439 (1996).
24. N. K. M. N. Srinivas, S. V. Rao, and D. N. Rao, "Saturable and reverse saturable absorption of Rhodamine B in methanol and water," J. Opt. Soc. Am. B **20**(12), 2470–2479 (2003).
25. P. C. Beaumont, D. G. Johnson, and B. J. Parsons, "Photophysical properties of laser-dyes - picosecond laser flash-photolysis studies of rhodamine-6g, rhodamine-b and rhodamine-101," J. Chem. Soc., Faraday Trans. **89**(23), 4185–4191 (1993).
26. M. Enescu, K. Steenkeste, F. Tfibel, and M.-P. Fontaine-Aupart, "Femtosecond relaxation processes from upper excited states of tetrakis(N-methyl-4-pyridyl)porphyrins studied by transient absorption spectroscopy," Phys. Chem. Chem. Phys. **4**(24), 6092–6099 (2002).
27. P. J. Gonçalves, P. L. Franzen, D. S. Correa, L. M. Almeida, M. Takara, A. S. Ito, S. C. Zílio, and I. E. Borissevitch, "Effects of environment on the photophysical characteristics of mesotetrakis methylpyridiniumyl porphyrin (TMPyP)," Spectrochim. Acta [A] (accepted), doi:10.1016/j.saa.2011.05.012.

1. Introduction

The optical properties of molecules are determined mainly by their electronic structure and dynamics, and thus, it is of great interest to investigate their electronic states from both fundamental and practical point of views. The importance of gathering information on the intersystem crossing time (τ_{isc}) and the triplet state quantum yield (φ_{isc}) was addressed many times in the literature [1–3]. For instance, the photosensitizer used in photodynamic therapy (PDT) is excited to a triplet state and this excitation can be transferred to a molecular oxygen (O_2), promoting it to a highly reactive singlet state. This activated oxygen will perform the citotoxic action required to kill tumor cells. Obviously, the efficiency of the therapy depends on the amount of photosensitizers transferred to the triplet state, which justifies the importance of studying the intersystem crossing process.

In addition to medical applications of this kind, a number of materials present suitable multilevel states that lead to resonant nonlinear optical processes. These processes, known as saturable absorption (SA) and reverse saturable absorption (RSA), can be exploited for the development of optical devices. SA is usually employed to produce pulsed lasers while most of the optical limiting devices are based on materials that present RSA. In this case, the molecule is promoted to a triplet state that absorbs more than the ground-state, limiting the amount of the light transmitted. Therefore, as in PDT, one of the relevant parameters to be studied is the triplet state quantum yield [4,5] Besides, the determination of the triplet state dynamics is also needed for the understanding of several processes, such as light harvesting [6,7], optimization of organic light emitting diodes (OLEDs) performance and to improve the efficiency of laser operation [8]. More recently, the triplet state was also found to be an important asset for achieving optical modulation and bistability [9].

Because of the several potential applications of compounds with high triplet yields, new methods that allow mapping the electronic states are welcome. The beforehand knowledge of

#144955 - $15.00 USD Received 28 Mar 2011; revised 14 May 2011; accepted 15 May 2011; published 18 May 2011

these quantities allows narrowing the list of candidates for a given application, allowing the choice of those with the best properties. One of the most traditional methods to measure the triplet excited-state parameters is based on the flash photolysis technique [10] and on its laser version that is capable of monitoring processes from microsecond to femtosecond time-scales [11]. Basically, this method works with a strong pump pulse and a delayed weak beam, which probes the absorption spectrum as a function of time. In this case, a few specific molecules with simple energy diagrams and photochemical processes can be well characterized in term of their triplet formation. Several other methods were introduced to improve the measurement of the photophysical parameters. For instance, time-resolved calorimetric methods, such as photoacustic calorimetry (PAC) and thermal lensing (TL), were shown to be sensitive enough to directly detect the heat released through nonradioactive processes of excited molecules. The PAC uses a deconvolution of the acoustic waves based on computer simulation and comparison between simulated and observed waves [12,13]. The signal generated by the heat-release pathway is characterized by lifetimes in the range from 10 ns to 20 μs. The TL is based on a two-color pump-probe scheme to provide information on the dynamics of molecules in the excited-state by monitoring the thermal lens signal [14,15]. Both PAC and TL are especially powerful for the investigation of nonfluorescent molecules and do not distinguish if the origin of nonradioactive processes is from singlet or triplet states. They are very useful when coupled to another technique capable of providing spectroscopic information on the nature of the transients, such as the LFP. Besides, all these techniques need a reference standard molecule with a known quantum yield. In the same way, by using the pulse train Z-scan technique [16] to study the nonlinear refraction or absorption [17], one can determine the molecule's excited-state cross-sections and dynamics. Gonçalves and associates demonstrated that this technique is also a suitable tool to investigate the triplet state quantum yield [18–20]. Additionally, pulse trains are also very useful in improving the hyper-Rayleigh technique to determine molecular hyperpolarizabilities [21]. In the pulse train Z-scan technique, however, several excited-states parameters are needed to fit the experimental data and this procedure may bring some uncertainty to the values obtained. One of the reasons for the large number of parameter involved is due to the fact that both ground- and excited-states of the singlet and the triplet states contribute to the nonlinear absorption. Instead of measuring the absorption, the fluorescence signal can also be used to characterize the spectroscopic parameters. In this case, some of the excited-state parameters can be neglected, reducing the number unknown variables in the experimental data analysis. By using two or more picoseconds pulses, Reindl *et al.* [22,23] have developed a time-resolved fluorescence method to study the population dynamics of the singlet-triplet states where they could also measure the quantum yield of triplet formation.

The present work introduces a method where the fluorescence induced by a set of pulses produced by a Q-switched and mode-locked Nd:YAG laser is explored to determine the excited-state dynamics. This pulse train fluorescence (PTF) technique presents several advantages over previous methods. For example, it allows determining the intersystem crossing time and the triplet state quantum yield with just one adjustable parameter, increasing the accuracy of the value measured. As each pulse in the train has its own irradiance value, they present an intrinsic irradiance scan provided they can be individually discriminated. Because the laser is Q-switched and mode-locked, it presents considerable smaller pulse-to-pulse power fluctuation than that of a single Q-switched laser, resulting in a better signal to noise ratio. Moreover, the pulse train allows measuring the fluorescence as a function of time and irradiance with a single beam configuration, without any delay stage and need to overlap the "pump" and "probe" pulses. The PTF technique brings two limitations: it does not work with samples that do not fluoresce and it does not give information about excited-state cross-sections.

In order to demonstrate the feasibility of the present technique, we performed PTF measurements in a few fluorescent molecules. We started with the well-known rhodamine B

#144955 - $15.00 USD Received 28 Mar 2011; revised 14 May 2011; accepted 15 May 2011; published 18 May 2011

(RB) molecule dissolved in methanol because population transfer to the triplet state is negligible and so, it can be used to visualize how the fluorescence of a pulse train behaves for a pure SA process. Here, one needs just the RB fluorescence time to adjust the experimental curves. Next, the triplet formation process was investigated through the fluorescence evolution in different porphyrins and the parameters obtained were compared to those obtained with different techniques, already published in literature. We also measured two porphyrins whose intersystem crossing times were not studied yet.

2. Materials and methods

Figure 1(a) presents a diagram of the experimental setup. As light source we used the second harmonic of a Q-switched and mode-locked Nd:YAG laser that delivers trains of 70-ps pulses at 532 nm. Each train contains approximately 25 pulses, separated by 13.2 ns, spanning a range of about 300 ns. The beam was focused into the sample (S) with a lens (L) of focal length f = 12 cm, producing a focal spot size whose diameter was about 50 μm. The sample was placed in a 2 mm-thick quartz cuvette. The fluorescence signal was collected perpendicularly to the excitation beam through a large core (1 mm diameter) optical fiber (OF) positioned close to the fluorescent spot. The optical fiber directed the fluorescence to a ~500 ps rise time silicon detector (D_1) which was fast enough to resolve the fluorescence decay. To avoid 532 nm scattered light, we used a long pass filter (Schott OG-590). A second fast detector (D_2) was used to monitor the pump pulse train that served as reference to calculate the normalized fluorescence (NF), defined as the ratio between the fluorescence and the reference signal, but with the initial value renormalized to one. This double-normalization can be justified on the basis that the initial pulses of the envelope (very small irradiance) do not induce cumulative processes related to the triplet state. In other words, the population of the triplet state is negligible for the first few pulses. Each peak height of the reference signal is proportional to the corresponding pulse fluence because the detection system has a rise time much slower than the 70 ps pulse duration. Both signals are averaged and recorded simultaneously in a 1 GHz digital average oscilloscope. The experiment and calculations were performed by softwares specially developed for those purposes. The measurement of a NF curve takes approximately 1 minute, basically due to the averaging process. Typical fluorescence (red) and reference (black) waveforms, acquired from the oscilloscope, are exhibited in Fig. 1(b). As seen, each individual fluorescence pulse presents an exponential decay that can provide the fluorescence lifetime of the compound. It is important to mention that lifetimes shorter than or of the order of the detector response time cannot be evaluated with the present technique.

The Gaussian beam parameters, w_0 and z_0, were carefully determined by performing *Z*-scan measurements in the well-characterized nonlinear material CS_2 [16], while the average power of the pulse train was measured with a calibrated power meter With these parameters, one can determine the fluence of each pulse of the envelope at the sample by using $w(z) = w_0[1 + (z/z_0)^2]^{1/2}$, where z is the distance between the sample and the focus, z_0 is the Rayleigh range and $w(z)$ is the beam spot size at the sample position.

#144955 - $15.00 USD Received 28 Mar 2011; revised 14 May 2011; accepted 15 May 2011; published 18 May 2011

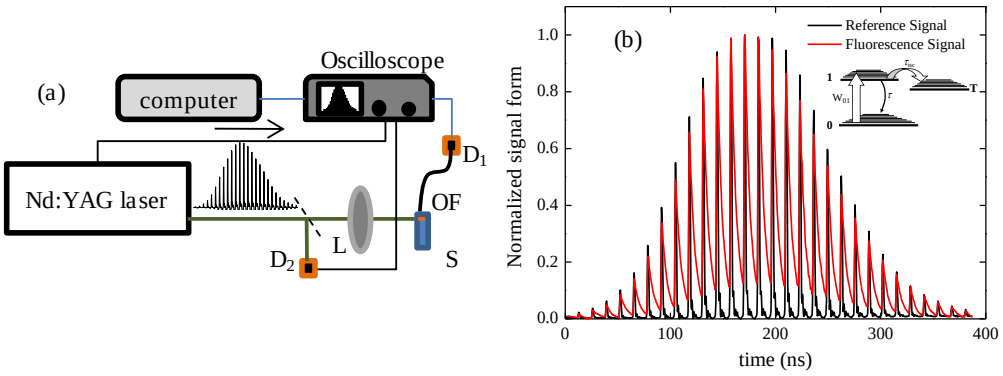

Fig. 1. (a) Diagram of the experimental setup. L: lens; D_1 and D_2: detectors; S: sample; OF: optical fiber. (b) Typical waveform obtained for fluorescence signal (red) and reference signal (black). The inset shows the three-energy-level diagram used to simulate the experimental results is shown.

With the purpose of getting a good insight on the technique, we measured the well-known fluorescent sample RB dissolved in methanol. This sample was already extensively studied, and most of its spectroscopic properties are known [24]. We prepared three different solutions, with concentrations of 1×10^{-3}, 1×10^{-4} and 1×10^{-5} Mol/l. The more diluted sample was used to measure the absorbance spectrum with a Cary 17 spectrophotometer, thus providing the ground-state absorption cross-section at 532 nm, found to be σ_{01} (532 nm) $\cong 24 \times 10^{-17}$ cm^2 [ε(532 nm) $\cong$ 64000 (M × cm)$^{-1}$], which is in agreement with the result reported elsewhere [25]. The pulse train measurements were carried out at different average powers, sample positions and laser repetition rates. After the fluorescence measurement, the linear absorption spectrum was taken again to verify if any sample degradation took place.

We have also performed PTF measurements in porphyrins with known intersystem crossing times. The samples studied are the free-base *meso*-tetra(sulfonatophenyl) porphyrin ($TPPS_4$), at pH 4 and pH 7, and the Zinc *meso*-tetra(sulfonatophenyl) porphyrin ($ZnTPPS_4$). The results were compared with those obtained by other methods [18–20]. Additionally, we measured two other samples, the free-base *meso*-tetrakis(4-N-methyl-pyridiniumyl) [26,27] (TMPP) and the Zinc *meso*-tetrakis(4-N-methyl-pyridiniumyl) (ZnTMPP) porphyrin [26], for which no information about their intersystem crossing times were found in the literature. All measurements were carried out in a concentration of about 1×10^{-4} Mol/l, using Milli_Q quality water as solvent.

The population dynamics resulting from the sample interaction with the pulse train can be understood with the aid of the three-energy-level diagram presented in the inset of Fig. 1(b). According to this model, when the first pulse of the envelope arrives, it promotes molecules from the ground singlet state (0) to the first excited singlet state (1). Molecules at the excited-state can relax back to the ground-state with a characteristic time, τ, which includes radiative and nonradiative interconversion processes, or relax to the triplet state (T) with an intersystem crossing time τ_{isc}. The population of higher excited singlets or triplets states can be neglected because, in general, their lifetimes are much shorter than the pulse duration. Additionally, when molecules undergo the intersystem crossing, they stay in the triplet state for a relatively long time, normally much longer than the time of the entire duration of the pulse train. Consequently, when the next pulse of the train arrives, the sample is in a different condition because part of the population was transferred to the triplet state. This cumulative mechanism repeats itself until the last pulse of the envelope excites the sample. Therefore, during the pulse train excitation, the fluorescence tends to decrease as pulses of the train reach the sample because of the ground-state depopulation. Since the singlet state lifetime and ground-state absorption cross-section can be determined by separate measurements, the only

#144955 - $15.00 USD Received 28 Mar 2011; revised 14 May 2011; accepted 15 May 2011; published 18 May 2011

adjustable parameter needed to fit the pulse train fluorescence signal is the intersystem crossing time.

As mentioned earlier, the reference signal is used to calculate the irradiance of each pulse of the envelope that acts in the sample. The population dynamics for each pulse of the envelope can be calculated through the following rate equations:

$$\frac{dn_0(t)}{dt} = -n_0(t)W_{01} + \frac{n_1(t)}{\tau} = -n_0(t)W_{01} + \frac{n_1(t)}{\tau_f} - \frac{n_1(t)}{\tau_{isc}}, \quad (1)$$

$$\frac{dn_1(t)}{dt} = +n_0(t)W_{01} - \frac{n_1(t)}{\tau_f}, \quad (2)$$

$$\frac{dn_T(t)}{dt} = \frac{n_1(t)}{\tau_f}, \quad (3)$$

where the transition rate is given by $W_{01} = \sigma_{01}I/h\nu$, and the lifetime of the first excited-state, measured through the fluorescence, is defined as $\tau_f^{-1} = \tau^{-1} + \tau_{isc}^{-1}$. h is the Planck constant, and ν is the photon frequency. n_i are the population fractions in each state. This set of rate equation can be numerically solved for each pulse of the train, considering also the population relaxation between pulses. This allows fitting the experimental data, which is proportional only to the population of the first excited singlet state. However, we also developed an analytical solution to the rate equations in a format that can be used more directly to analyze the data obtained with the pulse train. In order to do it, we considered that the pulse duration is much shorter than the relaxation times and neglected these when each pulse is present. In this case, upon the incidence of the j^{th} pulse of the train, with a known fluence F_j, the ground state is depleted by a factor $\exp\{-\sigma_{01}F_j/h\nu\}$, while the excited singlet state increases its population by $[1-\exp\{-\sigma_{01}F_j/h\nu\}]$ and the population of the triplet state remains constant. Between two consecutive pulses, W_{01} is zero and only relaxation occurs. In this case, the population of the excited singlet state decays by a factor $\exp\{-T/\tau_f\}$, and the ground and triplet states gain populations according to $(1-\tau_f/\tau_{isc})(1-\exp\{-T/\tau_f\})$ and $(\tau_f/\tau_{isc})(1-\exp\{-T/\tau_f\})$ respectively. Here, T = 13.2 ns is the time between two consecutive pulses of the train. By combining the two processes (laser on and off), one gets expressions relating the populations of the j^{th} and $(j\text{-}1)^{\text{th}}$ pulses:

$$(n_1)_j = \left(1-e^{\frac{-\sigma_{01}F_j}{h\nu}}\right)(n_0)_{j-1} + \left\{\left(1-e^{\frac{-\sigma_{01}F_j}{h\nu}}\right)\left(1-\frac{\tau_f}{\tau_{isc}}\right)\left[\left(1-e^{-\frac{T}{\tau_f}}\right)+e^{-\frac{T}{\tau_f}}\right]\right\}(n_1)_{j-1}, \quad (4)$$

$$(n_0)_j = e^{\frac{-\sigma_{01}F_j}{h\nu}}(n_0)_{j-1} + \left[e^{\frac{-\sigma_{01}F_j}{h\nu}}\left(1-\frac{\tau_f}{\tau_{isc}}\right)\left(1-e^{-\frac{T}{\tau_f}}\right)\right](n_1)_{j-1}, \quad (5)$$

Since the fluorescence is proportional to n_1 and the pulse fluence along the train is known, one can map the PTF along the train, as shown in Figs. 2(a)–2(c) for different fluorescence and intersystem crossing times. One can clearly see how the PTF envelope distorts for different values of these parameters. Alternatively, these results can be normalized to the fluence of the pulses, giving rise to the results of Figs. 2(d)–2(f). These simulations were achieved using the same input parameters, namely: σ_{01} = 2 x10^{-17} cm^2, laser power average of 5 mW, at 3 cm from the focus and the same reference signal (open stars in Figs. 2(a)–2(c)).

Figure 2 illustrates several situations that can be measured with the present technique. We considered three different cases of fluorescence lifetimes, for which the intersystem crossing times were changed. In Fig. 2(a), one can observe that for τ_{isc} of the order of the fluorescence

#144955 - $15.00 USD Received 28 Mar 2011; revised 14 May 2011; accepted 15 May 2011; published 18 May 2011

lifetime, the signal tends to decrease (see □). In this case, the NF is near zero for pulses at the end of the envelope, meaning that the population in the first excited-state is transferred to the triplet state and does not contribute to the fluorescence. In circumstances where τ_{isc} is longer than τ_f, the relaxation back to the ground-state and to the triplet state are both probable. In this situation, the population in the first excited-state can also return back to the ground-state. It means that all pulses will produce a certain fluorescence signal and the simulations show that the pulses at the end of the envelope present a residual fluorescence. This can be observed in Figs. 2(a)–2(c) for the cases ○ and △. A similar behavior, but even more enhanced, is observed if τ_{isc} is much longer than τ_f. In this case, the intersystem crossing process becomes less probable than the relaxation to the ground-state and the fluorescence signal is observed for all pulses with a higher magnitude that the case analyzed before (see (◁) and (▷)).

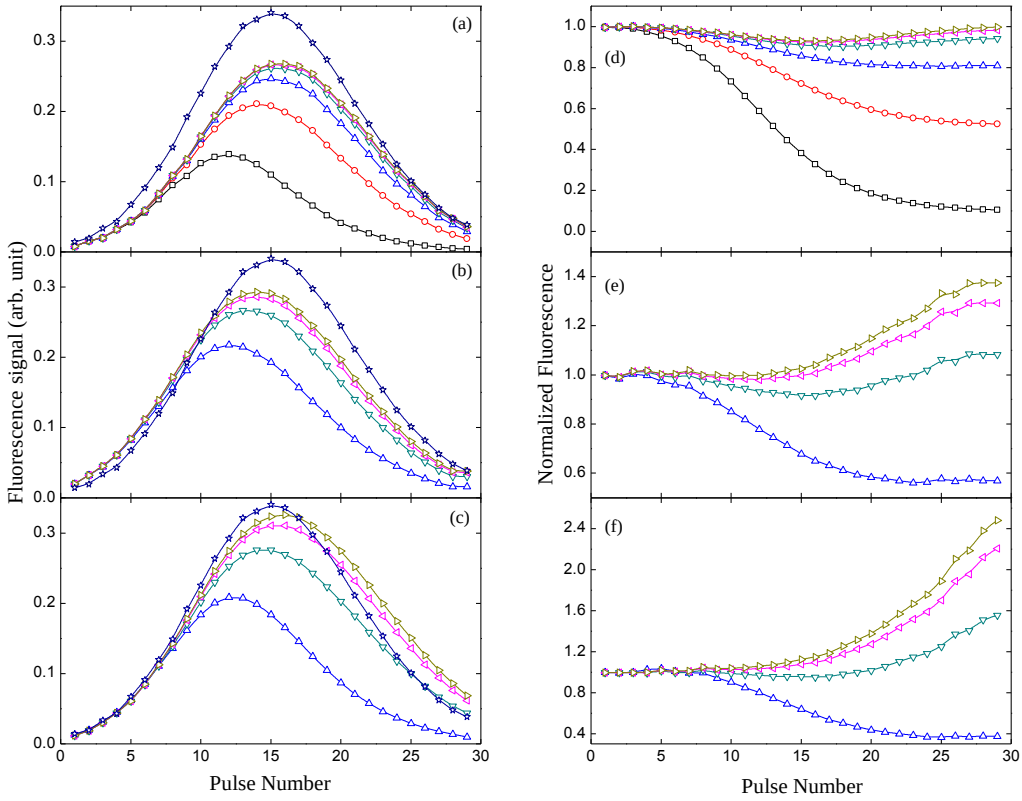

Fig. 2. (a), (b) and (c) depict the fluorescence signal envelope distortion for three different cases, in which the fluorescence time (τ_f) is kept constant as (a) 3 ns, (b) 13 ns and (c) 30 (ns). For these cases, the intersystem crossing time (τ_{isc}) is changed for each individual τ_f in the following order: 3 ns (□), 10 ns (○), 30 ns (△), 100 ns (▽), 300 ns (◁) and 1000 ns (▷). The open stars represent the pulse irradiance envelope shape just as reference for the reader. (d), (e) and (f) show the normalized fluorescence signal for the same cases as mentioned before. The simulations are only allowed when the $\tau_{isc} \geq \tau_f$.

The NF simulations that can be compared to the experimental results, even with different input parameters, are Fig. 2(d) (▷) and Fig. 2(d)(○) Fig. 2(e)(△), in which the first matches the rhodamine trend and the other two correspond to porphyrin cases. The first follows the same shape observed for rhodamine, although with a different magnitude (see Fig. 3(b), 8 mW). In the second case, one can observe a monotonic depletion of the fluorescence signal down to a constant value, much higher than zero (see Fig. 5).

#144955 - $15.00 USD Received 28 Mar 2011; revised 14 May 2011; accepted 15 May 2011; published 18 May 2011

3. Results and discussion

Figure 3(a) depicts the maxima of the excitation pulse train (open circles) and the corresponding peaks of the fluorescence signal (closed circles), obtained for the RB/methanol solution (concentration of 1×10^{-5} Mol/l), using an average power of 8 mW. Such dye is suitable to calibrate our technique since most of spectroscopic parameters are well known. The pulse number in Fig. 3(a) is arbitrarily labeled according to the pulse sequence. Here, the repetition rate of the laser was set to 100 Hz, and the sample was placed at 6.5 cm away from the focal point. Such position, arbitrarily chosen, gave good fluorescence signal. As Fig. 3(a) shows, the profile of the fluorescence envelope does not follow that of the excitation beam. We have also performed experiments with repetition rates from 5 Hz to 500 Hz and verified that it does not affect the fluorescence signal, indicating that thermal effects are not important. In addition, we also used different sample's positions and confirmed that it does not affect the parameters measured. To better analyze the results obtained for RB, Fig. 3(b) presents NF profiles for several excitation powers. The solid lines are fittings obtained with the three-energy-level diagram using the known spectroscopic parameters of RB, such as the fluorescence lifetime (~2.6 ns) and the intersystem crossing time (1 μs) [24]. Moreover, additional measurements indicated that the fluorescence parameters do not depend on the concentration. Using a fixed average power, the excitation rate can also be played by changing the sample position with respect to focal point. However, in this case, special attention should be taking on fluorescence detection geometry to avoid changes on the fluorescence collection during sample scan.

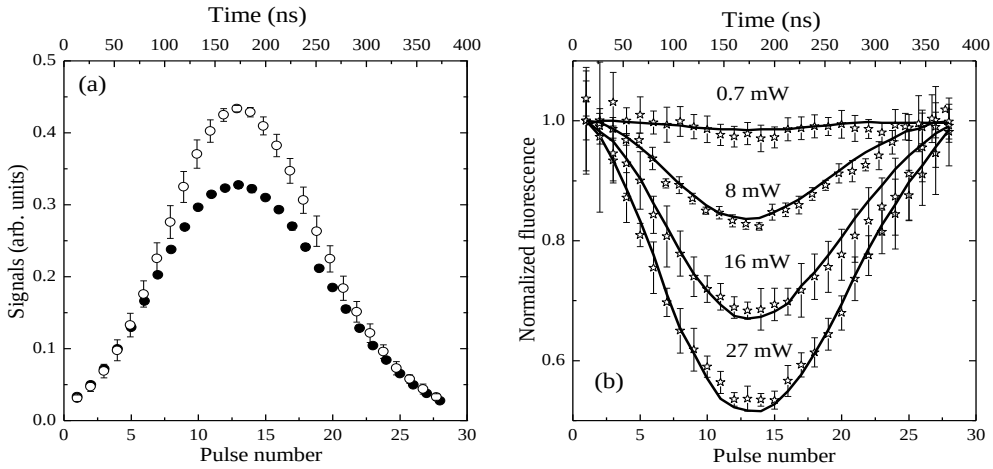

Fig. 3. (a) Reference (open circles) and fluorescence (closed squares) signals measured at a power of 8 mW in rhodamine B solution. (b) NF signal for different laser power. The solid lines are the discreet simulations obtained with the three-energy-level diagram, using the known RB spectroscopic parameters.

The PTF clearly shows a saturation effect along the Q-switch envelope because the pulses in central part of the train are stronger than those at the border of the Q-switch envelope and the fluorescence signal suffers a reduction due to the ground-state depletion. Regardless of the existence of any excited-state absorption, the ground-state population is not recovered and fewer photons are scattered by unit time, inducing the fluorescence saturation. As the laser power decreases, the ground-state population is recovered because there is no transfer to the triplet state and the NF returns to a value close to 1. These effects are conveniently described by the rate equations, as seen by the solid lines in Fig. 3(b). Although we used a tabulated value for the RB fluorescence lifetime, the present technique also provides this parameter for fluorescent compounds whose time is longer than the response time of the detector (~500 ps).

#144955 - $15.00 USD Received 28 Mar 2011; revised 14 May 2011; accepted 15 May 2011; published 18 May 2011

As seen in Fig. 1(b), each fluorescence peak of the envelope presents an exponential decay that can be fitted to provide the fluorescence lifetime. However, in order to show, in a clear way, the fluorescence decays curves from the compounds studied here, we used a pulse picker (Pockels Cell) to extract an unique pulse from the Q-switched and mode-locked envelope. With this single pulse, at 100 Hz repetition rate, we are able to observe the entire fluorescence decays without the interference of the other pulses of the envelope. It can be visualized in Fig. 4, which shows, in an expanded time, the fluorescence decays of TMPP, TPPS pH 7 and 4, ZnTMPP and $ZnTPPS_4$ and also their respective fittings with exponential function (solid lines). Additionally, the detector response (dotted line) is also plotted to compare with the fluorescence signals. For $ZnTPPS_4$ and ZnTMPP, that present the fastest decays, we obtained 1.7 ± 0.2 and 1.3 ± 0.2 ns, respectively. These parameters are used to calculate the intersystem-crossing time. The other fluorescence decay times are listed in Table 1. If the fluorescence lifetime is of the order of the detector response, a mathematic deconvolution algorithm must be used to evaluate this time.

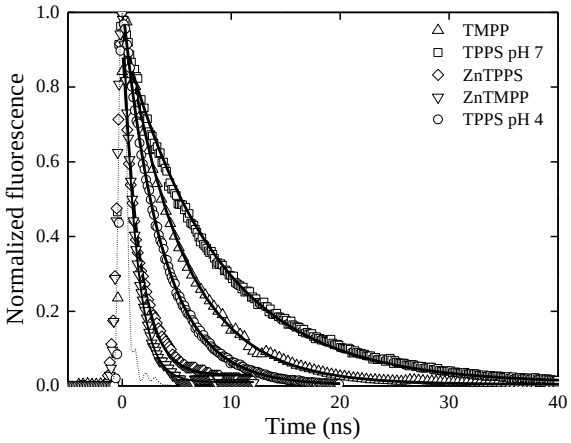

Fig. 4. Normalized fluorescence decays of different porphyrins studied in this work. The solid lines represent a simple exponential fitting. The dotted line corresponds to the reference waveform.

In order to investigate the triplet state dynamics and to determine the intersystem crossing time, we carried out measurements in two distinct free-base porphyrins and in two Zn porphyrins, some of them with well characterized triplet states information ($TPPS_4$ and $ZnTPPS_4$). Figures 5(a) and 5(c) present the NF for free base *meso*-tetra(sulfonatophenyl) porphyrin ($TPPS_4$) at pH 4 [18,19] and Zn *meso*-tetra(sulfonatophenyl) porphyrin ($ZnTPPS_4$) [20] respectively, both dissolved in Milli-Q water, measured for two different laser power at 3 cm from the focus. One can observe that as the pulse number increases, the NF decreases until it reaches a constant value. Such behavior is different than the one presented in Fig. 3(b) for RB.

At the beginning of the train, the NF signal follows the same trend as for rhodamine B - a decrease in the normalized fluorescence signal. However, close to the highest intensity pulse, the fluorescence signal does not recover as RB does. This can be explained by considering that the population in the first excited-state does not return entirely to the ground-state, but is also transferred to the long lived triplet state due to the intersystem crossing process. Once in the triplet state, these molecules are trapped there for a long lifetime, ceasing to fluoresce. Using the spectroscopic parameters obtained by means of the absorbance spectra and fluorescence decays like those of Fig. 4, we applied the three-energy-level diagram depicted in the inset of Fig. 1(b) to determine the intersystem crossing time. The fittings (solid lines) are in good agreement with the experimental curves (open circles). We obtained values for the intersystem-crossing time of τ_{isc} = 9.8 ± 0.4 ns and τ_{isc} = 2.5 ± 0.4 ns for $TPPS_4$ at pH4 and

#144955 - $15.00 USD Received 28 Mar 2011; revised 14 May 2011; accepted 15 May 2011; published 18 May 2011

$ZnTPPS_4$ respectively, showing a good agreement with the values reported in the literature [18–20]. Furthermore, changes in laser power do not affect the intersystem crossing time, as expected. Consequently, both curves in Fig. 5(a) and also in Fig. 5(c) are adjusted with the same parameters, having only a distinct laser power. The difference observed for the NF values is due to the population transferred to the triplet state. Once the laser power increases, the population in the triplet state also increases, and, as a consequence, the fluorescence signal decreases faster.

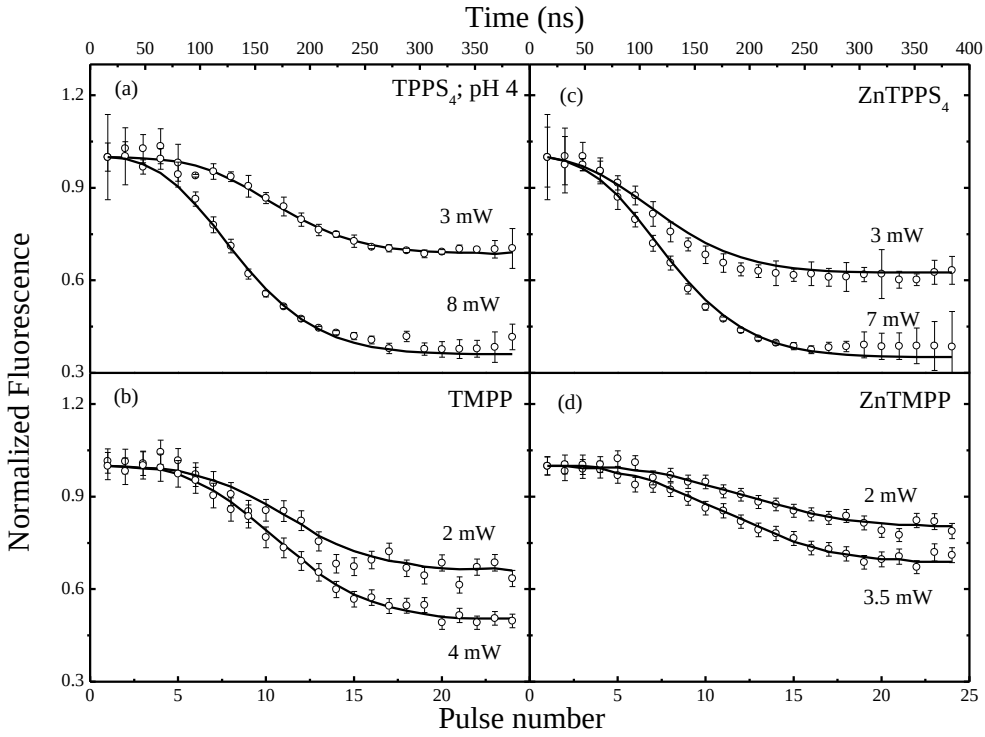

Fig. 5. Normalized fluorescence (open circles) for 4 different porphyrins measured at different laser power and at 3 cm sample position with respect to the focal plane. The solid lines are the discreet simulation obtained with the three-energy-level diagram and the values shown in Table 1.

Following the same procedure, we used the technique to characterize the intersystem crossing process of two new porphyrins. In Figs. 5(b) and 5(d), we show the results for the free base *meso*-tetrakis(4-N-methyl-pyridiniumyl) (TMPP) and Zn *meso*-tetrakis(4-N-methyl-pyridiniumyl) (ZnTMPP) dissolved in Milli-Q water. The measurements were carried out using different laser powers (2 mW and 4 mW for TMPP and 2 mW and 3.5 mW for ZnTMPP) at 3 cm from the focal plane. Again, one can observe a reduction in the fluorescence as a function of the pulse number in the envelope. The solid lines are the fittings obtained using the rate equations Eqs. (1)–(3). In this case, we obtained $\tau_{isc} = 8.0 \pm 1$ ns for the free base TMPP and $\tau_{isc} = 2.0 \pm 0.5$ ns for the ZnTMPP. Table 1 presents the parameters used and obtained in the fittings. Additionally, the triplet quantum yields formation, which is defined as $\varphi_{isc} = \tau_f / \tau_{isc}$, are also shown. Besides, Table 1 also depicts the values (a) obtained from [18–20], which demonstrates a good agreement between different techniques.

#144955 - $15.00 USD Received 28 Mar 2011; revised 14 May 2011; accepted 15 May 2011; published 18 May 2011

Table 1. Spectroscopic Parameters Used and Calculated for the Porphyrins

	σ_{10}	τ_f (ns)	τ_{isc} (ns)		φ(isc)	
	This Work	This Work	This Work	a	This Work	a
$TPPS_4$ pH4	0.8 ± 0.1	3.5 ± 0.4	9.8 ± 0.4	10	0.37 ± 0.09	0.36
$TPPS_4$ pH7	2.1 ± 0.1	9.6 ± 0.5	13.1 ± 0.6	13	0.74 ± 0.08	0.77
$ZnTPPS_4$	1.7 ± 0.1	1.7 ± 0.4	2.5 ± 0.4	2.3	0.7 ± 0.1	0.74
TMPP	3.0 ± 0.1	5.4 ± 0.5	8 ± 1	-	0.67 ± 0.08	-
ZnTMPP	1.5 ± 0.1	1.3 ± 0.3	2.0 ± 0.5	-	0.7 ± 0.1	-

[a]Values obtained from [18–20]. The absorption cross-section (σ_{10}) is given in (1×10^{-17} cm^2).

4. Conclusions

In summary, we have developed a new method to measure excited state spectroscopic properties of molecules by time-resolved fluorescence induced by Q-switched and mode-locked train of pulses at 532 nm. The theoretical analysis was made with a simple three-energy-level and the corresponding rate equations. An analytical solution for the rate equations was also proposed. Singlet saturable absorption, intersystem crossing time and triplet yield formation could be obtained by fitting the experimental data with the proposed model. Here, we were able to quantify such spectroscopic parameters of rhodamine B and four different porphyrins. This single beam, background free and low noise method was proven to be very simple and precise. We believe that the central idea of this technique, which lies in the cumulative nature of some spectroscopic signal, can be explored using other types of pulse sequences generated by other methods, such as a multipass cavity, once several pulsed lasers (even frequency tunable) are readily available.

Acknowledgments

We acknowledge the support of the Fundação de Amparo à Pesquisa do Estado de São Paulo and the Conselho Nacional de Desenvolvimento Científico e Tecnológico. We also thank to Dr. Carlos Toro for helpful discussions.

#144955 - $15.00 USD Received 28 Mar 2011; revised 14 May 2011; accepted 15 May 2011; published 18 May 2011